

DAS microseismic monitoring feasibility study at the Newberry volcano geothermal site

Ismael Vera Rodriguez¹, Trenton Cladouhos², Thomas Coleman¹, Carlos Maldaner¹ and David Podrasky¹

¹Silixa LLC

²Mazama Energy Inc

Summary

The feasibility of microseismic monitoring using Distributed Acoustic Sensing with two downhole fibers is analyzed at the Newberry volcano geothermal site. One of the wells in this study is preexisting and the second is in plans to be drilled and stimulated. The study consists in generating a spatial grid of synthetic DAS seismograms informed by previous studies to define the potential microseismic source mechanism and event distances from the fibers. Furthermore, the noise signals in each of the fibers are implemented through the incorporation of real noise records from a previous acquisition in a similar setting. These real records are scaled in consideration to regions of the boreholes where the fibers are expected to be cemented and uncemented. The analysis of the noisy synthetic data provides information about areas of reduced sensitivity around the boreholes, location errors influenced by the borehole geometries, and the range of magnitudes of events that could be detected with one or more direct seismic arrivals in individual boreholes. The latter determines whether events are detectable but not locatable (single-phase detections) or detectable and locatable (two or more phases detections). The results from this analysis are useful to inform the planning of the new well trajectory in additional consideration of its target area for stimulation, as well as the form of deployment of the fibers.

Background

The Newberry volcano site located in Oregon, USA is a geothermal field where very hot rocks (>350°C) are accessible relatively close to the surface (Bonneville et al., 2021). Through Enhanced Geothermal Systems (EGS), the heat from these hot rocks can be more optimally utilized to meet energy demands. As part of these efforts, Mazama Energy Inc is planning the drilling of a new injection well on the west flank of the caldera. The well head is located on the same pad of an existing borehole that runs deviated in an eastward direction. The current proposal for the deviation survey of the new well also runs in the same plane of the existing well but starts with a westward deviation before correcting direction towards the east (Figure 1). Hydroshearing of the nearby formation will be induced from the new well at an approximate depth of 4,100 m. Microseismic monitoring using DAS will be deployed to aid in the determination of the stimulated volume, and to verify that the magnitude of induced seismicity remains within safe levels.

With the purpose of maximizing sensitivity to the microseismic signals of interest, the current proposal for fiber deployment considers Silixa's Constellation™ engineered fibers. In the case of the existing well, the fiber could be deployed down to a measured depth (MD) of approximately 2,750 m. From surface to a MD of 1,970 m the fiber would hang inside cemented casing, and after that, inside an uncemented blank liner. Inside the new well, the fiber would be hanging from surface down to a MD of approximately 1,220 m, and after that, it would be cemented behind the casing down to a MD of 2,590 m (see Figure 1).

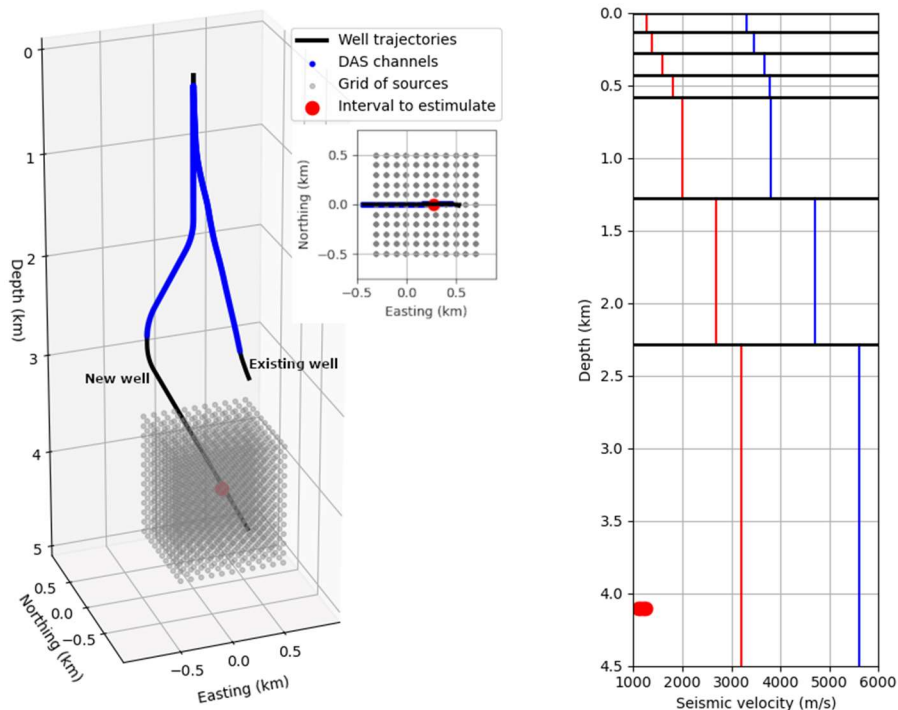


Figure 1. Left panel: geometries of the wells (black lines) where the DAS fibers (blue lines) will be deployed and the grid of microseismic sources (grey points) considered for the feasibility study. The inset is a map view showing that the well paths are contained within an EW plane. Right panel: distribution of P-wave (blue) and S-wave (red) velocities used to generate synthetic DAS seismograms. In both panels red markers denote the central depth of the interval from where hydroshearing will be induced.

Studies of microseismicity observed during previous EGS-related stimulations in the Newberry volcano site have reported microseismicity at distances within 1 km from the injection well (Cladouhos et al., 2013, Aguiar and Myers, 2019). These analyses used records from a network of seismic stations located inside shallow boreholes and directly on the surface. As a result of the geometry of the monitoring array, the estimated event locations displayed significant uncertainties in their vertical coordinate (Templeton et al., 2014). In terms of detectability, the surface stations appear to have a limit of detectability around $M_w 0.8$, while the sensors located inside the shallow boreholes could detect microseismicity down to about $M_w 0.0$ (Cladouhos et al., 2013). More detailed analysis using Matched Field Processing and template-based detection discovered additional lower signal-to-noise-ratio (SNR) microseismic signals. Although these events fell within a similar range of magnitudes of the originally detected catalogue, the magnitude of completeness of the sensor network nevertheless lowered from $M_c=0.7$ to $M_c=0.3$ by increasing the number of the lower magnitude detections (Templeton et al., 2014, 2020). As it is known that the surface network (and also likely a DAS fiber) are sensitive to the minimum event magnitude considered safe to continue operations ($M_w \sim 2$, Cladouhos, 2013), this feasibility study focuses on the minimum magnitude of events that could be detected with the proposed DAS arrays.

In terms of source mechanisms, previous microseismic studies at Newberry report source types ranging from opening cracks, through pure double couples and closing cracks (Cladouhos, 2013). A detailed study by Aguiar and Myers (2019) pointed at different stress regimes in shallow and deep areas of the site, with the predominant source type below 2.6 km being normal faulting.

With respect to velocity distributions in the area of study, ambient noise interferometry with records from the surface network has been used to construct 1D and 3D velocity models (Matzel et al., 2014). From a 1D model that contained only compressional velocities and using as a reference the mean V_p/V_s ratios over varying depths observed in the 3D velocity model, we constructed a 1D model to use in this study (Figure 1, right panel).

Methodology

The feasibility study used a grid of seismic sources with separations of 100 m between them. The grid was centered at the position planned for hydroshearing in the new well. The maximum source offset from this central point was 500 m in horizontal directions and 600 m in the vertical direction (see Figure 1). Synthetic distributed strain seismograms were then modeled from each grid source to DAS channels located at the proposed intervals of the existing and new wells. The DAS channels were simulated at spacings of 10 m. Similarly, the gauge length used to recreate DAS seismograms was also set to 10 m. The sampling interval in the synthetic seismograms was set at 1 ms. For the source time function, we used a Brune pulse with corner frequency of 80 Hz. The seismic moment in the source mechanism was normalized such that synthetic seismograms could be scaled to study detectability for different event magnitudes. The source mechanism in all the synthetic sources was specified as normal-faulting (i.e., dip-slip) double-couples striking at 60° azimuth, consistent with the study from Aguiar and Myers (2019).

Detectability was investigated by incorporating noise records from a previous DAS microseismic monitoring survey conducted at the FORGE geothermal underground lab (Lellouch et al., 2020). These records were acquired with the same type of Constellation™ engineered fiber proposed for the Newberry site cemented behind the casing. To accommodate the above-described fiber deployment conditions at Newberry and the parameters used for the feasibility study, the FORGE records were first decimated in their channel spacing to 10 m. For channels corresponding to depths between the surface and 1,970 m MD in the existing well, the noise records were boosted 10 dB in amplitude, for the remaining channels the boost was increased to 20 dB. In the case of the new well, noise records for DAS channels located between the surface and a MD of 1,220 m were boosted by 10 dB, while noise records for channels below this depth were left unchanged. The modifications in noise amplitudes are based on experience and meant to approximate noise levels considering the expected conditions of deployment of the fiber in each well. The modified real noise records were then added to the DAS synthetic seismograms previously scaled to simulate varying event magnitudes and input to a detection algorithm based on root-mean-square (RMS) stacks (Figure 2). In this way, we used the results to analyze areas of lower event detectability, the minimum event magnitude that could be detected from individual boreholes, and minimum event magnitude for events that could also be located.

Location was investigated with clean synthetics. For this purpose, every source in the grid was located using a migration stack method. The location process was conducted in two ways: one

considering a full 3D space and the second using a 2.5D approach. Given the symmetry plane formed by the well deviations, it was expected that 3D locations could not be fully constrained, thus, the 2.5D approach was implemented to investigate an alternative form of event location more appropriate to the monitoring geometry.

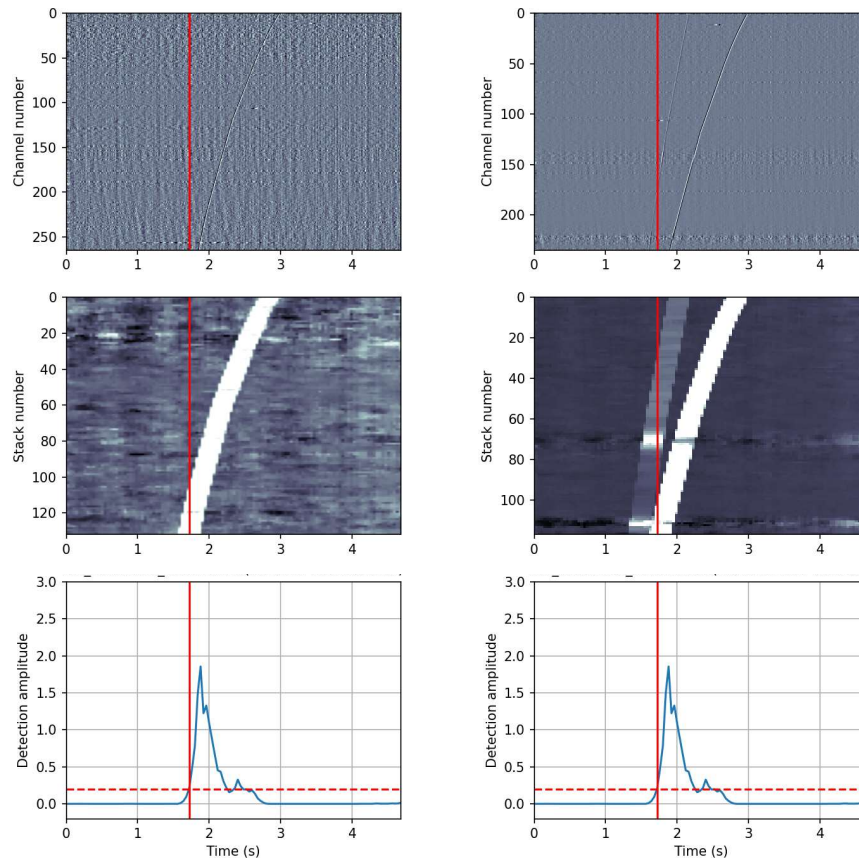


Figure 2. Example of noisy DAS synthetic seismograms prepared for this study. From top to bottom are the time domain records, RMS panels, and a joint detection function. Left and right panels display data for the existing and new wells, respectively. Red vertical lines are detection times and red-dashed horizontal lines the triggering threshold. The event magnitude in this case is M_w -0.25.

Results

- **Detectability and locatability of microseismic events**

Using DAS channels from the existing well and event magnitudes of M_w 0, the RMS-based algorithm was able to detect events from 97% of the modeled volume, out of which 44% were locatable (i.e., events where P and S arrivals were above the noise level). Reducing to M_w -0.25, the detectability volume reduced also to 59% with only 5% of locatable events. At M_w -0.5 no events were detected with the RMS method. Detectability is lost first in the bottom southwest section of the modeled volume (Figure 3), while locatability is more likely for locations near the

top northwest and southeast sections (Figure 4). Better detectability is achieved with DAS channels from the new well, where 98% of the volume displays detectability for Mw-0.75. In this case, detectability disappears in all the volume for Mw-1.25. On the other hand, locatability is worse for similar levels of detectability, as only 24% of the volume shows locatability for Mw-0.75. For DAS channels in the new well, detectability disappears first from the top northeast and bottom west sections of the modeled volume (Figure 3). Locatability, on the other hand, is more likely for events in the northwest and southeast sections (Figure 4). Joint processing of the two-well data improves mostly locatability but only when the phase arrivals are above the noise level in the existing well data. For instance, with Mw-0.75, about 97% of the volume shows detectability with 24% of locatable events displaying at least 2 phase arrivals above the noise level and less than 1% displaying at least 3 phase arrivals above the noise level. These are practically the same results obtained with data from the new well alone. On the other hand, with Mw-0.5 the detectability remains in about 97% of the volume, but the locatable region with at least 2 phase arrivals above the noise increases to 84%, and with at least three phase arrivals increases to 21%. Figures 3 and 4 present distributions of the regions of detectability and locatability for selected Mw using individual and joint processing of the two-well data.

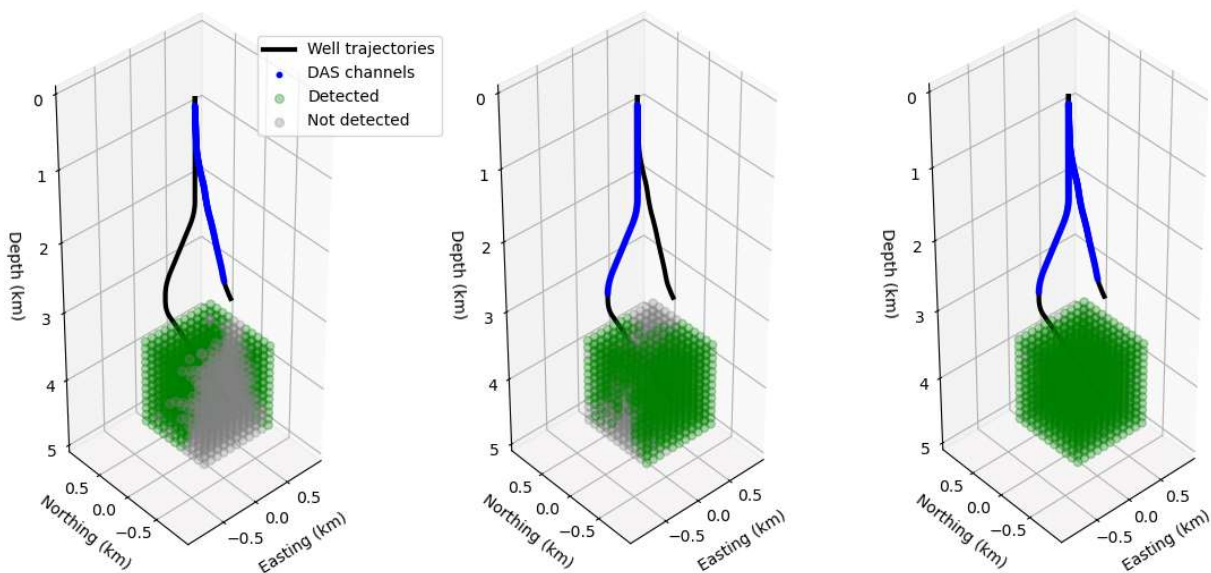


Figure 3. Regions of detectability (green dots) for different modeled magnitudes and DAS channels processed. Left: DAS channels in the existing well with Mw-0.25 (59% detectability). Middle: DAS channels in the new well with Mw-1 (55% detectability). Right: DAS channels in both wells with Mw-0.75 (97% detectability).

- **Location errors**

Locations in a 3D space are unconstrained in the north-south direction, this is, perpendicular to the plane of symmetry formed by the well trajectories. This is equally observed for locations estimated with DAS channels from one well or with both wells processed together (Figure 5). This lack of constraint results in epicentral errors of more than 300 m irrespective of whether individual

well data is processed separately or if data from both wells is processed together. Vertical positions on the other hand are better constrained but errors are still larger than 160 m whether data from both wells is processed individually or jointly. By reducing the location solution space to two coordinates (i.e., easting and depth), and a distance normal to the symmetry plane (i.e., 2.5D locations), epicentral errors are reduced to a median of 100 m, and depth errors to 15 m for the case of joint processing. These error estimations are best case scenarios estimated with noiseless seismograms and with a perfect knowledge of the velocity model of the medium. Additional error can be expected depending on the SNR in the data and the inaccuracies inherent to the actual velocity model used for processing.

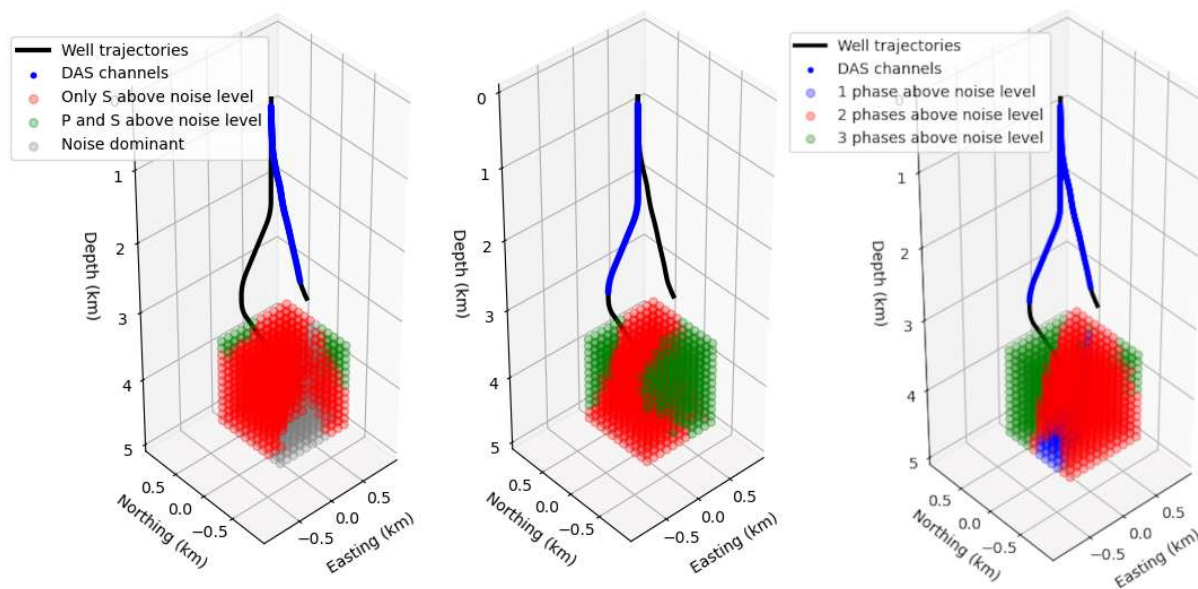


Figure 4. Distribution of sources with phase arrivals above the noise level for different modeled magnitudes and DAS channels processed. Left: DAS channels in the existing well with Mw-0.25 (5% locatability). Middle: DAS channels in the new well with Mw-0.75 (24% locatability). Right: DAS channels in both wells with Mw-0.5 (84% locatability with at least two phase-arrivals above the noise level). Notice that the legend is only different for the right panel.

Discussion and conclusions

DAS microseismic feasibility in the Newberry volcano site shows that microseismic activity could be detected down to Mw-0.75 with a Constellation™ DAS array placed at the new well. However, only about 24% of the region within ~500 m around the stimulated point may produce events detected with both P and S phases above the background noise, this is, locatable events at this magnitude level. Higher Mw is needed to increase the region of locatable events. In the case of DAS channels in the existing well, the lower SNR also increases detectability levels to Mw-0.25. At Mw0, detectability is similar to that of the new well at Mw-0.75 but more events detected in the existing well at this magnitude (44%) present locatable events with both P and S phases above

the noise level. These results are influenced by the source mechanism of the seismic sources and the form of deployment of the fibers that was considered. Thus, significant variations of the source radiation pattern with respect to that considered here will also modify the regions of detectability and locatability. On the other hand, the noise levels in actual records can be uncertain. The noise scaling used for this study is conservative and any changes that lower the noise floor, particularly in the existing well, would help to lower the magnitude of events that are both detectable and locatable using a joint processing of both well DAS data.

Epicentral location errors are significant in 3D estimates because of the symmetry plane formed by the well deviations. Limiting the location solution space to one half north or south of this plane, improves the epicentral estimates. Compared to uncertainties observed in previous location estimates using the surface sensor network, it becomes clear that a combined processing of surface and downhole records would produce the best outcome with a better epicentral constraint given by the surface network and a better depth constraint given by the downhole DAS records.

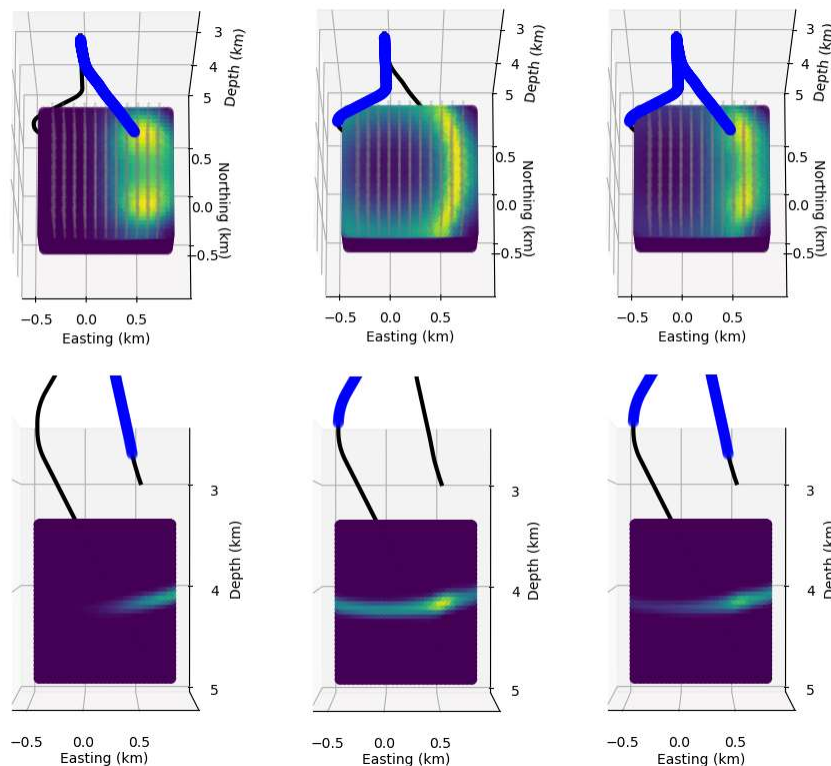


Figure 5. Example 3D location probability volumes generated for one source location in the northeast of the modeling domain. Notice the symmetric amplitude anomaly generated in the southwest of the probability volumes as a result of the monitoring geometry in all cases. From left to right are results using DAS data from the existing well, the new well, and a combination of both, respectively. The estimation of 2.5D locations uses only one half (north or south) of the solution domain, which removes the ambiguity.

Acknowledgements

We are thankful to Mazama Energy Inc for granting permission for the publication of these results.

References

Aguiar, A. and Myers, S. (2019). Microseismic focal mechanisms and implications for changes in stress during the 2014 Newberry EGS stimulation, *Bull. Seismol. Soc. Am.*, **109**, 1653-1660.

Bonneville, A., Asanuma, H., Cladouhos, T., Friðleifsson, G., Horne, R., Jaupart, C., de Natale, G., Noren, A., Petty, S., Schultz, A. and Sørli, C. (2021). The Newberry super-hot EGS project. Proceedings World Geothermal Congress, Reykjavik, Iceland.

Cladouhos, T., Petty, S., Nordin, Y., Moore, M., Grasso, K., Uddenberg, M., Swyer, M., Julian, B. and Foulger, G. (2013). Microseismic monitoring of Newberry volcano EGS demonstration. Proceedings 38th Workshop on Geothermal Reservoir Engineering, Stanford CA, USA.

Lellouch, A., Schultz, R., Lindsey, N., Biondi, B. and Ellsworth, W. (2021). Low-magnitude seismicity with a downhole distributed acoustic sensing array – Examples from the FORGE geothermal experiment, *Journal of Geophysical Research: Solid Earth*, **126**, e2020JB020462.

Matzel, E., Templeton, D., Petersson, A. and Goebel, M. (2014). Imaging the Newberry EGS site using seismic interferometry. Proceedings 39th Workshop on Geothermal Reservoir Engineering, Stanford CA, USA.

Templeton, D., Johannesson, G., and Myers, S. (2014). An investigation of the microseismicity at the Newberry EGS site. Proceedings 39th Workshop on Geothermal Reservoir Engineering, Stanford CA, USA.

Templeton, D., Wang, J., Goebel, M., Harris, D. and Cladouhos, T. (2020). Induced seismicity during the 2012 Newberry EGS stimulation: Assessment of two advanced earthquake detection techniques at an EGS site, *Geothermics*, **83**, 101720.